

FABRICATION OF HIGH- T_c HOT-ELECTRON BOLOMETRIC MIXERS FOR SUBMILLIMETER HETERODYNE APPLICATIONS

M.J. Burns, A.W. Kleinsasser, B. Karasik, M. Gaidis, and W.R. McGrath

*Center for Space Microelectronics Technology, Jet Propulsion Laboratory,
California Institute of Technology, Pasadena, CA 91109, USA*

Abstract

Superconducting hot-electron bolometers are the most promising candidate for heterodyne mixers at frequencies above 1 THz. These devices operate by heating of electrons in the superconductor, and thus have no energy gap related frequency limitation, such as exists in SIS mixers, for example. Nb hot-electron bolometric mixers have recently demonstrated superior performance to competing Schottky mixers at frequencies above 1 THz, but of course must be operated at liquid helium temperatures. $\text{YBa}_2\text{Cu}_3\text{O}_{7-\delta}$ hot-electron bolometric mixers introduce the possibility of sensitive, low power heterodyne detectors operating at temperatures approaching 90 K for high-background applications, such as earth observing missions. We describe the fabrication of high- T_c devices based on ultrathin (<20 nm) $\text{YBa}_2\text{Cu}_3\text{O}_{7-\delta}$ films for use as 2.5 THz mixers.

Introduction

Heterodyne receivers based on superconductor-insulator-superconductor junctions for use in submillimeter astronomical and atmospheric studies at frequencies up to 1 THz have been produced [1,2]. At higher frequencies, Schottky diode mixers or direct detection techniques are generally used. Superconducting hot-electron bolometers (HEB), consisting of a thin film microbridge, have been proposed for use in heterodyne applications in the terahertz (THz) range [3,4]. Superconducting hot-electron bolometric mixers require orders of magnitude less local oscillator power than semiconductor mixers, allowing for solid state local oscillators rather than the large lasers

required of Schottky diode mixers. Nb HEB mixers operating at 2-4 K have shown excellent performance at 530GHz [5], and recently demonstrated low noise at 1.2THz [6] and 2.5THz [7]. While some initial experiments on device physics and heterodyne performance [8,9] have been carried out on high-temperature superconductor (HTS) bolometric mixers, no optimized devices have been reported to date.

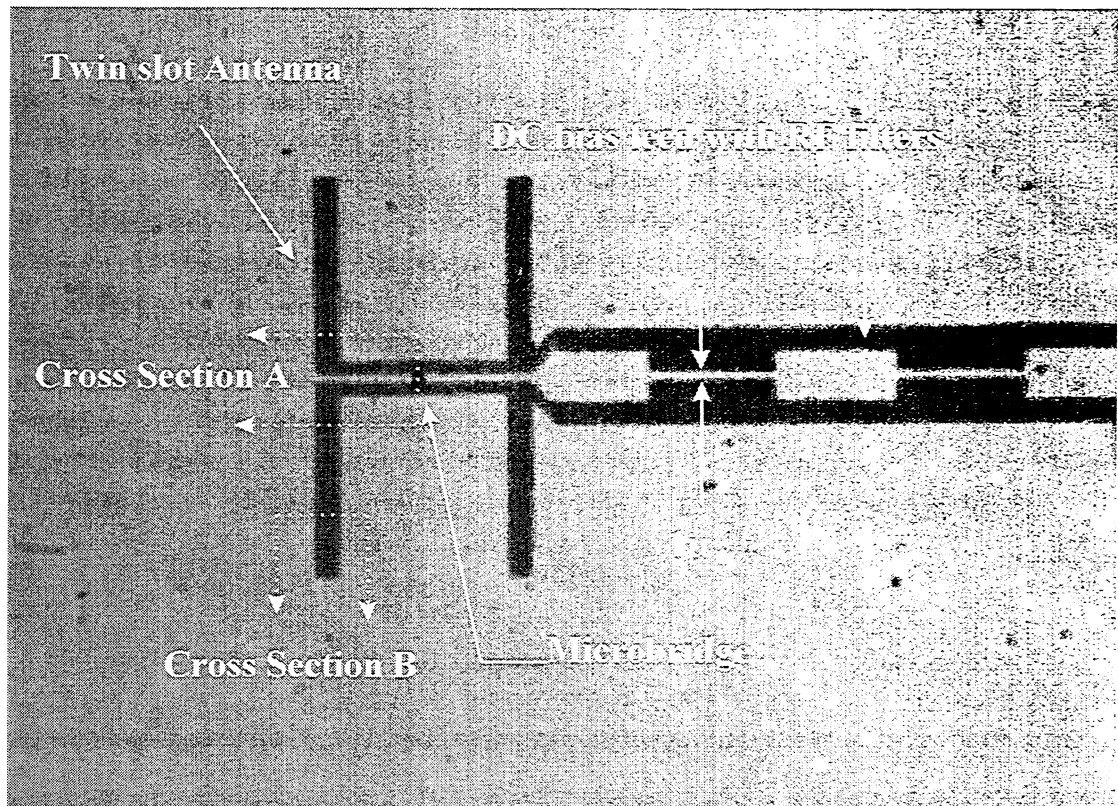


Figure 1 -- Finished 2.5THz hot electron bolometric mixer showing twin slot antenna, DC bias feed with filters, and the active element microbridge. Dark areas are where all material has been removed, thus exposing the dark substrate. Light areas are Au. Dashed lines show two cuts for the cross sections of Figure 3. Cross section A is across the twin slot and microbridge, cross section B is illustrative of the dark areas where the substrate is exposed.

The lower local oscillator power requirements of superconducting hot-electron bolometric mixers makes them particularly attractive for remote sensing

systems with constraints on the availability of power or mass, such as on balloon or space-based platforms. Hot-electron bolometric mixers made from HTS operating in the range of 60-85 K are particularly attractive for space based applications since they can be cooled with existing space qualified closed-cycle refrigerators.

In this paper we describe the fabrication of nominally of microbridge bolometers based on ultrathin (<20 nm) $\text{YBa}_2\text{Cu}_3\text{O}_{7-\delta}$ films for HEB mixer applications at 2.5 THz [10]. A photograph of a finished 2.5 THz twin-slot mixer with a $\text{YBa}_2\text{Cu}_3\text{O}_{7-\delta}$ device is shown in Fig. 1, and a microbridge connected to dc contact pads is shown in Fig. 2.

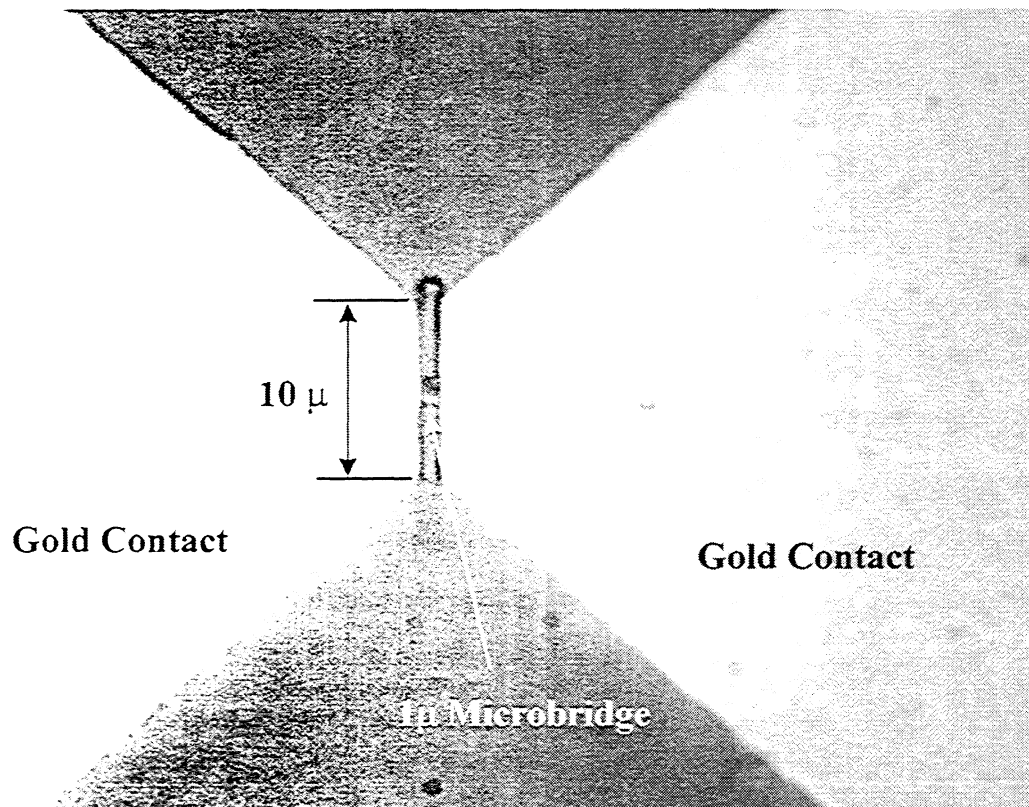


Figure 2 -- Finished microbridge located in the center of dc contact pads.

Requirements

The design and operating principles of our 2.5 THz HTS hot-electron bolometric mixer are described in detail elsewhere [10]. Hot-electron bolometric mixer operation depends on heating the electrons by the incoming rf radiation, resulting in a nonequilibrium energy distribution. Cooling occurs via electron-phonon interactions whereby the hot electrons give their energy to phonons which escape into the substrate. Alternatively, cooling can occur by diffusion of the hot electrons out of the device and into the normal-metal electrical contacts [4]. Due to the short electron mean-free-paths in HTS materials, the electron-phonon cooling mechanism dominates in HTS hot-electron bolometric mixers.

In space applications, system-level power restrictions constrain mixers to operate at low local oscillator power levels, with major implications for device size. As a result of these considerations, the major device design requirements [10] for HTS hot-electron bolometers are described below. The first four requirements pertain to the substrate. While a large number of substrates can individually meet these conditions, it is important for optimal mixer performance to meet all simultaneously.

The substrate must have a high thermal conductivity and be compatible with epitaxial $\text{YBa}_2\text{Cu}_3\text{O}_{7-x}$ (YBCO) growth. This requirement can be met by a number of substrates compatible with high-quality YBCO films. MgO , LaAlO_3 , Al_2O_3 and YAlO_3 have thermal conductivities at 90 K of 3.4, 0.35, 6.4 and 0.2-0.4 $\text{W K}^{-1} \text{cm}^{-1}$, respectively. For comparison, yttrium stabilized zirconia (YSZ) has a thermal conductivity at 90 K of only 0.015 $\text{W K}^{-1} \text{cm}^{-1}$ [10].

The thermal boundary resistance (R_b) between the HTS film and the substrate should be as small as possible. This second requirement can be met by several of the aforementioned substrates. The values of R_b , inferred from measurements of

the phonon escape time, between YBCO and MgO, LaAlO₃ and Al₂O₃ at 90 K are 5, 10, and 11 × 10⁻⁴ K cm² W⁻¹ respectively [11-15].

Substrates need to have a small loss-tangent at both 2.5 THz and at the IF frequency. This fourth requirement can also be met by a number of the aforementioned substrates. MgO, LaAlO₃, Al₂O₃ and YAlO₃ have loss tangents of 7, 5, 8, and 10, × 10⁻⁶, respectively at 90 K and ~10 GHz. For comparison, yttrium stabilized zirconia (YSZ) has a loss tangent of 400 × 10⁻⁴ at 90 K at ~10 GHz [10].

Substrates need to have a convenient dielectric constant at both 2.5THz and at the IF frequency. This fifth requirement can also be met by a number of HTS compatible substrate materials. The dielectric constants of MgO, Y₂O₃, Si-on-Al₂O₃ and YAlO₃, measured in a Fourier transform infrared spectrometer at JPL, are 10.0, 12.9, 9.9 and 21.2, respectively, at 77 K and 2.5 THz.

The film must be ultra-thin (10-20 nm) to minimize the phonon escape time and allow for optimum mixer performance at GHz IF's [10]. In addition, the HTS mixer film volume must be small enough to allow device operation at microwatt local oscillator power levels. This third requirement dictates that the mixer be constructed from films patterned to submicron dimensions [10].

In this work, ~20 nm YBCO thick films on YAlO₃ substrates were used to fabricate hot-electron bolometric mixers.

Growth and Patterning

Growth of the superconductor and gold (Au) contact layers are performed completely *in situ* without exposure of interfaces to the ambient environment. The devices are grown on 250 μm thick, 1x1cm² (001) YAlO₃ substrates polished on both sides. The nominal growth process is: The substrates are mounted on Haynes alloy plates using Ag paint. These are transferred into the HTS deposition system via a load-lock. The substrates are buffered using a 20 nm

PrBa₂Cu₃O_{7- δ} (PBCO) layer deposited by pulsed laser deposition at 790°C, 400 mTorr of O₂, at a fluence of 1.6 J/cm² at $\lambda=248\text{nm}$. Substrate are heated radiatively, and monitored by a thermocouple that is cross checked by an optical pyrometer prior to film growth. The PBCO layer is followed by a 20 nm YBCO layer deposited at 810°C, 200 mTorr of O₂, and 1.6 J/cm². The deposited bilayer is cooled *in situ* at 40°C/minute in a 500-650 Torr O₂ atmosphere from the growth temperature down to room temperature. Next 100 nm of Au is deposited *in situ* by DC magnetron sputtering in a 1 mTorr Ar atmosphere. The resulting trilayer structure is illustrated in Fig. 3a-i. Typical transition temperature (T_c) for these trilayers, as determined by AC susceptibility, is 83-86 K with a transition width of less than 2 K.

After the trilayer growth process, the substrate is mechanically removed from the Haines alloy plate. Photoresist (AZ5214) is spun onto the blank trilayers to a thickness of 1.5 μm and soft-baked at 95 °C for 2 minutes. The sintered Ag paste residue remaining from substrate mounting on the Haines plate is dry honed from the substrate with a razor, followed by swabbing with 100% HNO₃ and rinsing in water. The photoresist is then removed with acetone and the devices are rinsed in 100% ethanol and blow-dried with dry N₂.

The initial patterning of the PBCO/YBCO/Au trilayer into the antenna, RF filter, IF/DC contacts and bolometer microbridge is performed using optical contact lithography. Photoresist is spun onto the unpatterned trilayers to a thickness of 0.5 μm and soft-baked at 95°C for 2 minutes. The resist is exposed through a chrome contact mask and developed. The resist is soft-baked again at 95°C for 1 minute and ashed for 30 seconds in a 40 mTorr oxygen plasma in a Semi Group 1000TP reactive ion etch (RIE) tool at 120 watts, with a DC substrate self-bias of -320 volts [16]. The minimum feature size with good definition for this process is 1 μm .

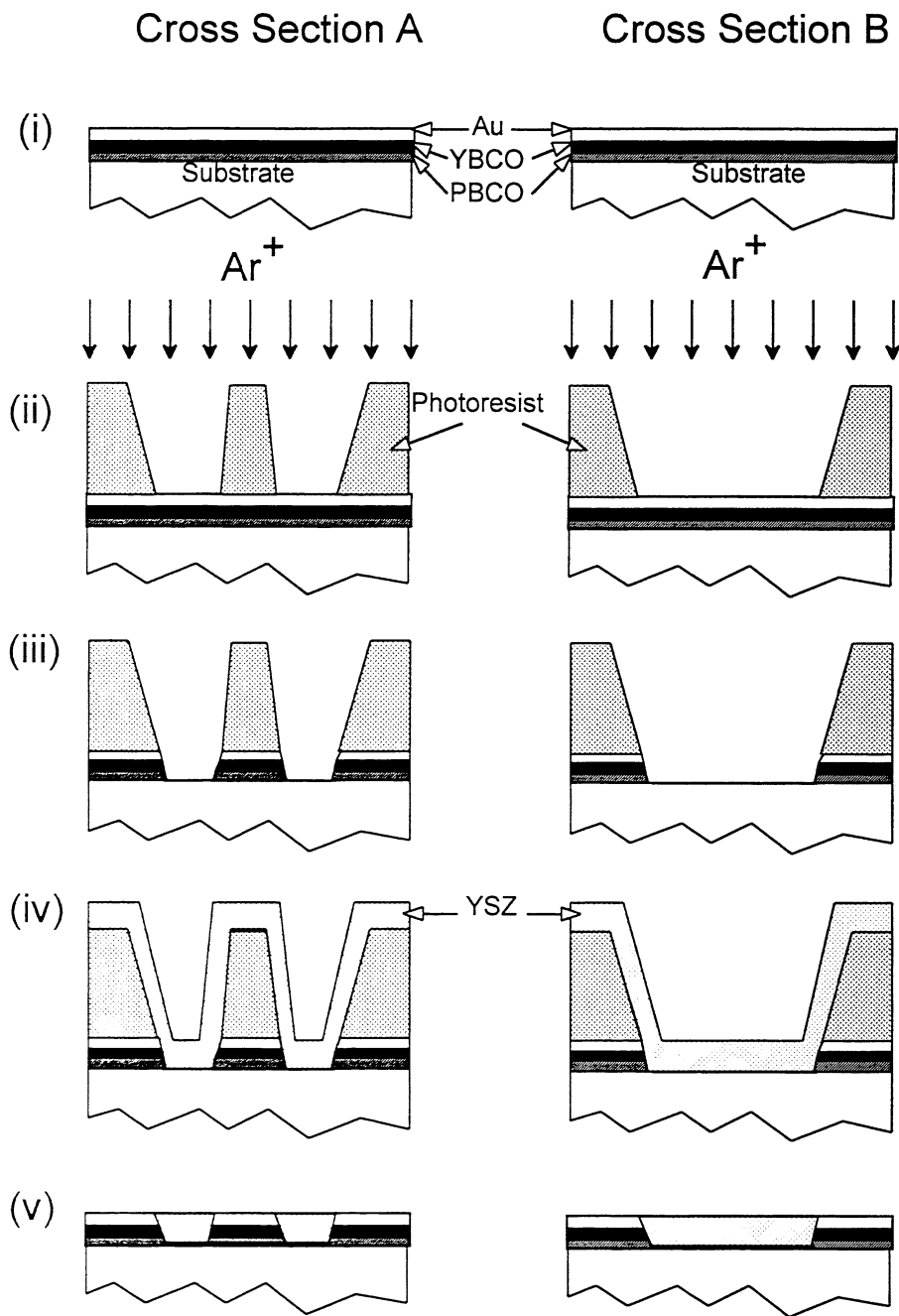


Figure 3a – First five process steps for cross sections A & B of the device in Fig. 1. The steps are described in the text.

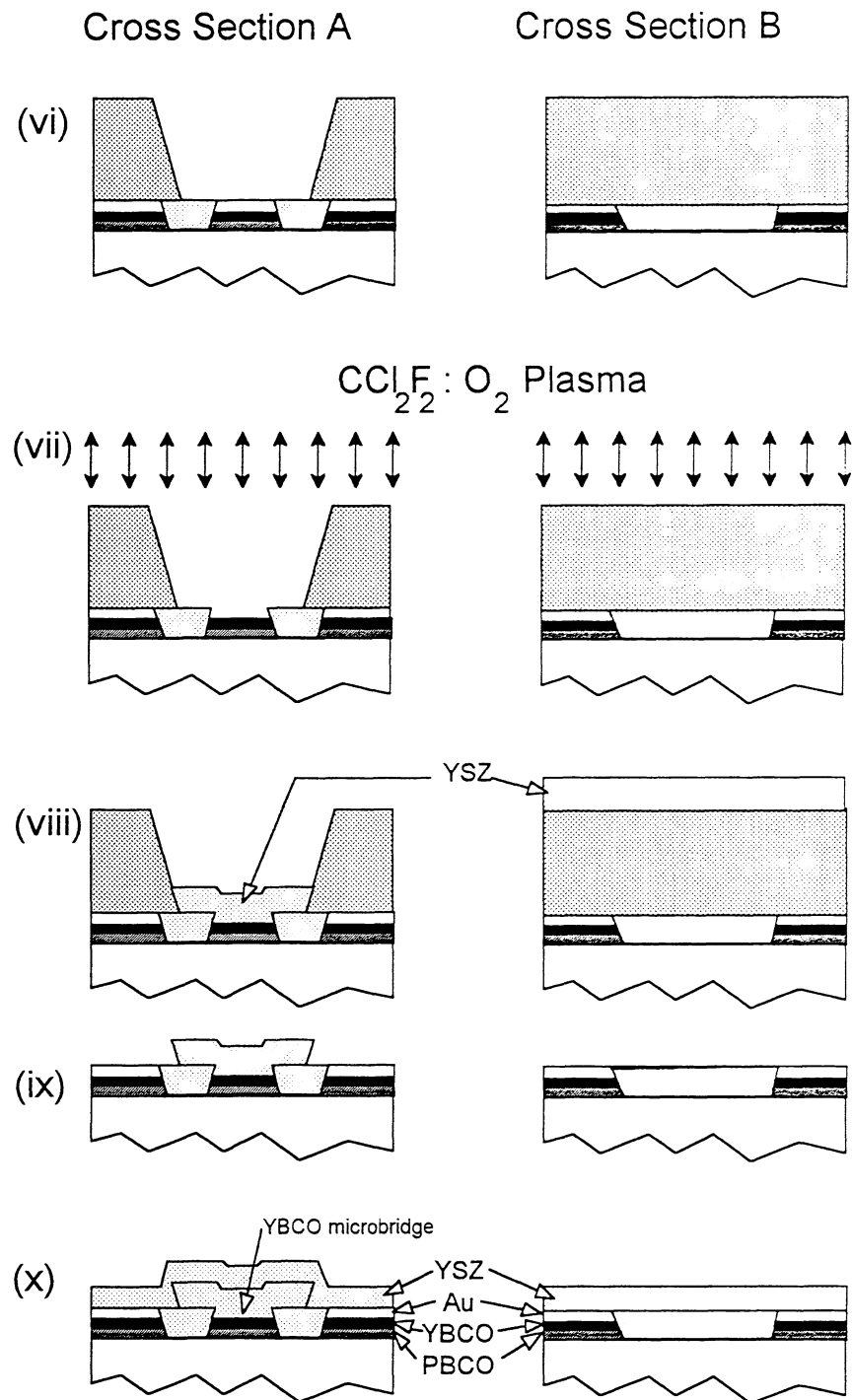


Figure 3b – Second five process steps for cross sections A & B of the device in Fig. 1. The steps are described in the text.

Next, the devices are placed into the load-lock of the deposition system in which an ion mill is located. The etching process uses normally incident 500 eV Ar⁺ ions at 1 mA/cm² for 5 minutes (Fig. 3a-ii). The pressure is 2.0x10⁻⁴ Torr. The substrates are not cooled, however the temperature remains below 100 °C during the etching process and no polymerization of the photoresist is observed. The resulting layer structure is illustrated in Fig. 3a-iii.

After milling, the devices are transferred from the load-lock directly into the deposition system where 60 nm of YSZ is deposited at room temperature by pulsed laser deposition, resulting in the layer structure shown in Fig. 3a-iv.

The photoresist is then removed by ultrasonically cleaning the devices in acetone for 1-2 minutes. The devices are rinsed in 100% ethanol and blow dried with dry N₂. The first resist layer is thus used for two purposes, the process of patterning the antenna and feed structure, and for a self-aligned step of capping device side walls with a YSZ layer, resulting in the layer structure shown in Fig. 3a-v.

At this point in the process, another layer of photoresist is spun on the device to a thickness of 0.5 μm, soft-baked, exposed, and developed using the procedure described above. The mask for this step opens a small window in the resist, exposing the 1 μm-wide bolometer bridge, which is still covered with 100 nm of Au as shown in Fig. 3b-vi. The device is then placed in the RIE system for the following procedure illustrated in Fig. 3b-vii: (1) Oxygen ashing for 5 minutes in a 200 mTorr oxygen plasma at 60 watts with approximately -80 self bias. (2) Etching for 50 minutes in a 200 mTorr 1:10 O₂:CCl₂F₂ plasma at 60 watts with approximately -20 volts self bias. The approximate Au removal rate is 2.5 nm/minute. We have found that over etching does not damage *c*-axis-oriented YBCO. (3) Oxygen ashed for 2 minutes in a 200 mTorr oxygen plasma at 30 watts with approximately -40 volts self bias. It should be noted that without the

YSZ side-wall coating covering the *a-b* plane edges of the YBCO layer, lines as wide as 50 μm are no longer superconducting after the Au RIE process, presumably due to chlorine being driven into the film along the *a-b* planes. With the YSZ side-wall coating, we have successfully used this 3-step Au removal process on 20 nm thick YBCO lines as narrow as 400 nm and maintained T_c above 80 K. Such a line test structure, and its superconducting transition are shown in Figure 4. However it should be noted that the yield on devices declines precipitously as the microbridge size drops below 3 μm^2 .

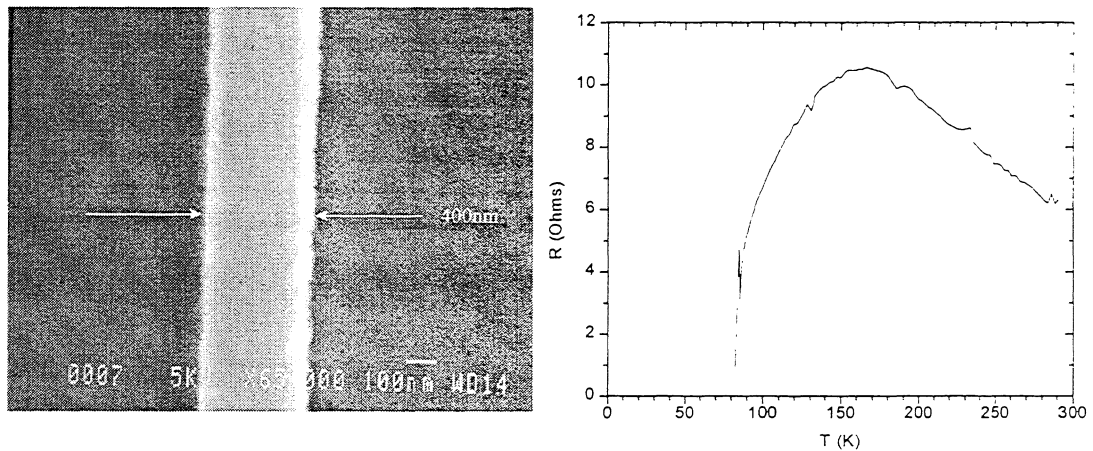


Figure 4 -- Narrow line (400nm wide) of 20nm thick YBCO after the Au removal process described in the text. Superconducting transition approximately 80K.

Next the devices are placed in the pulsed laser deposition system load-lock, pumped down and immediately transferred into the deposition chamber, where 100 nm of YSZ is deposited by pulsed laser deposition, filling in the area where the Au was just removed (Fig. 3b-viii). The total time from removal from the RIE to pumping down in the load lock is always less than 10 minutes, and typically less than 5 minutes. The photoresist is then removed by ultrasonically cleaning the devices in acetone for 1-2 minutes. The devices are rinsed in 100% ethanol

and blow dried with dry N₂. The resulting layer structure for the device after this process step is illustrated in Fig. 3b-ix.

The devices are next placed back into the deposition system where 100 nm of YSZ is deposited by pulsed laser deposition onto the entire substrate at room temperature. The resulting layer structure for the device after this final deposition step is illustrated in Fig. 3b-x.

Photoresist is next spun onto the 1x1cm² substrates (now containing 19 chips) to a thickness of 1.5 μm and soft-baked at 95 °C for 2 minutes. The substrates are mounted on a dicing saw and cut into individual chips. The photoresist is then removed with acetone and the devices are rinsed in 100% ethanol and blow dried with dry N₂. Photographs of a finished device in a twin-slot mixer is shown in Fig. 1, as is a simple microbridge with dc contacts in Fig. 2.

Electrical Tests

For DC device tests, individual die are mounted in 28-pin Keocera ceramic chip packages which plug into the bottom of a cryogenic dipping probe. Four wires are ultrasonically bonded to the YSZ-covered Au contacts. With proper settings, the wire bonds make contact through the nominally 100 nm thick YSZ over-layer. The wire bond connections are chosen in order to allow 4-terminal device measurements on the twin slot devices, eliminating resistance contributions from the probe and instrumentation wiring. The wire bond connections in the devices with dc contacts allow only 2-terminal measurements..

Resistance versus temperature measurements are taken using a computer controlled system. For some measurements, a Keithley 220 DC current source connected to two leads applies ±1 mA and the voltage response of the device under test is measured for both current polarities using an HP 3457A multimeter. The difference is used to eliminate contributions from thermally induced

voltages in the probe and instrumentation wiring. For other measurements a lock-in amplifier is used with a low frequency current source.

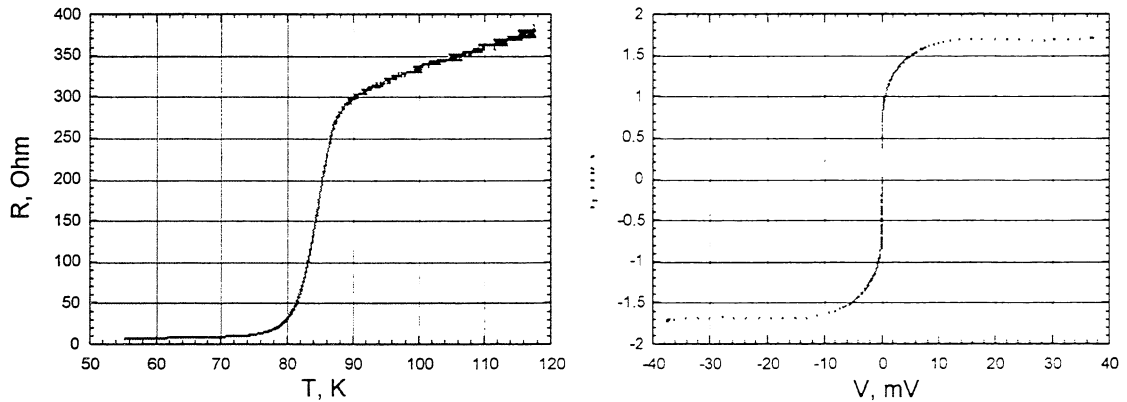


Figure 5 -- An R vs. T and a 77K I-V curve for a $1 \times 1 \times 0.02 \mu\text{m}^3$ microbridge with dc contacts of the type shown in Fig. 2. The R vs. T curve includes the 10Ω lead resistance.

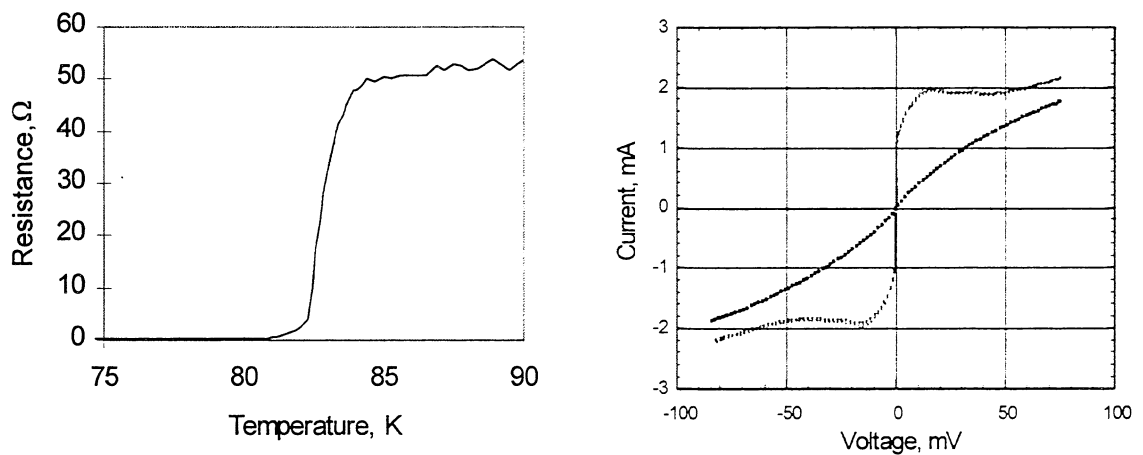


Figure 6 -- A R vs. T and an I-V curve with and without applied local oscillator power for a $1 \times 1 \times 0.02 \mu\text{m}^3$ microbridge in a 2.5Thz twin slot antenna as shown in Fig. 1.

After processing, the microbridge T_c determined from the R vs. T data is generally 2-3K lower than the T_c of the initial trilayer film measured by AC susceptibility. The transition widths are also slightly broader. Fig. 5 shows R vs. T and a 77K I-V curve for a $1 \times 1 \times 0.02 \mu\text{m}^3$ microbridge with dc contacts as shown in Fig 2. There is a baseline resistance of about 10 ohms from the probe wiring.

The samples are RF tested by mounting in an aluminum block and placed in an optical cryostat.[17] The 2.5 THz local oscillator consists of a methanol far-infrared laser, pumped by a $\lambda=9.6\mu\text{m}$ CO₂ laser. I-V curves at 77 K, with and without applied local oscillator power (estimated power absorbed in the device is about 100 μW), are also shown in Fig 6. With the application of local oscillator power, the critical current of the microbridge at 77 K can be almost entirely suppressed from its initial value of approximately $5 \times 10^6 \text{ A/cm}^2$.

Conclusion

We have designed and fabricated superconducting hot-electron bolometers based on a recently developed model [10]. The devices utilize ultra-thin YBCO ($\leq 20 \text{ nm}$) films patterned into $1\mu\text{m}$ by $1\mu\text{m}$ microbridges and passivated with YSZ. These bridges maintain T_c on the order of 80 K and J_c 's $> 1 \times 10^6 \text{ A/cm}^2$ at 77 K. We have demonstrated that the devices were successfully coupled to a 2.5 THz local oscillator source when operated at 77 K.

Acknowledgments

The authors thank L.P. Lee, B. Bumble, H.G. LeDuc and D.B. Tanner for useful discussions, and H.M. Pickett and T.J. Crawford for the 2.5THz Fourier transform infrared spectrometer substrate measurements. The research described in this paper was performed by the Center for Space Microelectronics Technology, Jet Propulsion Laboratory, California Institute of Technology, and

was sponsored by the National Aeronautics and Space Administration, Office of Mission to Planet Earth, and the Office of Space Science.

References

- [1] M. Bin. M.C. Gaidis, J. Zmuidzinas, T.G. Phillips, H.G. LeDuc, "Low-noise 1 THz niobium superconducting tunnel junction mixer with a normal-metal tuning circuit", *Appl. Phys. Lett.* **68**, 1714 (1996)
- [2] M. Bin. M.C. Gaidis, J. Zmuidzinas, T.G. Phillips, H.G. LeDuc, "THz SIS mixers with normal-metal Al tuning circuit", *Supercond. Sci. Tech.* **9**, A136 (1996)
- [3] E.M. Gershenzon, G.N. Gol'tsman, I.G. Gogidze, Y.P. Gusev, A.I. Elant'ev, B.S. Karasik and A.D. Semenov, "Millimeter and submillimeter range mixer based on electronic heating of superconducting films in the resistive state", *Sov. J. Supercond.* **3**, 1582 (1990)
- [4] D.E. Prober, "Superconducting terahertz mixer using a transition-edge microbolometer," *Appl. Phys. Lett.* **62**, 2119 (1993)
- [5] A. Skalare, W.R. McGrath, B. Bumble, H. G. LeDuc, P.T. Burke, A.A. Verheijen, R.J. Schoelkopf, and D.E. Prober, "Large bandwidth and low-noise in a diffusion-cooled hot-electron bolometer mixer", *Appl. Phys. Lett.* **68**, 1558 (1996)
- [6] A. Skalare, W.R. McGrath, B. Bumble, and H. G. LeDuc, "Receiver measurements at 1267 GHz using a diffusion-cooled superconducting transition-edge bolometer", to appear in the Proceedings of the 1996 Applied Superconductivity Conference (*IEEE Trans. Appl. Superconductivity*)
- [7] B. S. Karasik, M. C. Gaidis, W.R. McGrath, B. Bumble, and H. G. LeDuc, "A low-noise 2.5 THz superconductive Nb hot-electron mixer", to appear in the Proceedings of the 1996 Applied Superconductivity Conference (*IEEE Trans. Appl. Superconductivity*)
- [8] V.A. Trifonov, B.S. Karasik, M.A. Zorin, G.N. Gol'tsman, E.M. Gershenzon, M. Lindgren, M. Danerud, D.M. Winkler, "9.6mm wavelength mixing in a patterned $\text{YBa}_2\text{Cu}_3\text{O}_{7.8}$ thin film", *Appl. Phys. Lett.* **68**, 1418 (1996)
- [9] Yu. P. Gousev, A.D. Semenov, E.V. Pechen, A.V. Varlashkin, R.S. Nebosis, and K.F. Renk, "Coupling of terahertz radiation to a high- T_c superconducting hot electron bolometer mixer", *Appl. Phys. Lett.* **69**, 1 (1996)

- [10] B. S. Karasik, W.R. McGrath, and M. Gaidis, "Analysis of a high- T_c hot-electron superconducting mixer for terahertz applications", *J. Appl. Phys.* **81**, 1581 (1997).
- [11] G.L. Carr, M. Quijada, D.B. Tanner, C.J. Hishumugi, G.P. Williams, S. Estemand, B. Dutta, F. DeRosa, A. Inam, T. Venkatesan, and X. X. Xi, "Fast bolometric response by high- T_c detectors measured with subnanosecond synchrotron radiation", *Appl. Phys. Lett.* **57**, 2725 (1990)
- [12] N. Bluzer, "Temporal relaxation of nonequilibrium in Y-Ba-Cu-O measured from transient photoimpedance response" *Phys. Rev. B* **44**, 10222 (1991)
- [13] C.D. Marshall, I.M. Fishman, R.C. Dorfman, C.B. Eom, and M.D. Fayer, "Thermal diffusion, interfacial thermal barrier, and ultrasonic propagation in $\text{YBa}_2\text{Cu}_3\text{O}_{7-\delta}$ thin films: surface-selective transient-grating experiments", *Phys. Rev. B* **45**, 10009 (1992)
- [14] A.V. Sergeev, A.D. Semenov, P. Kouminov, V. Trifonov, I.G. Goghidze, B.S. Karasik, G.N. Gol'tsman, and E.M. Gershenzon, "Transparency of a $\text{YBa}_2\text{Cu}_3\text{O}_{7-\delta}$ -film/substrate interface for thermal phonons measured by means of voltage response to radiation", *Phys. Rev. B* **49**, 9091 (1994)
- [15] M. Danerud, D. Winkler, M. Lindgren, M. Zorin, V. Trifonov, B.S. Karasik, G.N. Gol'tsman, and E.M. Gershenzon, "Nonequilibrium and bolometric photoresponse in patterned $\text{YBa}_2\text{Cu}_3\text{O}_{7-\delta}$ thin films", *J. Appl. Phys.* **76**, 1902 (1994)
- [16] Reference herein to any specific commercial product, process, or service by trade name, trademark, manufacturer, or otherwise, does not constitute or imply its endorsement by the United States Government or the Jet Propulsion Laboratory, California Institute of Technology.
- [17] B.S. Karasik, M.C. Gaidis, W.R. McGrath, M.J. Burns, and A.W. Kleinsasser, To be published.